



## Sulfur poisoning and regeneration of the Ag/-Al<sub>2</sub>O<sub>3</sub> catalyst for H<sub>2</sub>-assisted SCR of NO<sub>x</sub> by ammonia

Doronkin, Dmitry E.; Khan, Tuhin Suvra; Bligaard, Thomas; Fogel, Sebastian; Gabrielsson, Pär; Dahl, Søren

*Published in:*  
Applied Catalysis B: Environmental

*Link to article, DOI:*  
[10.1016/j.apcatb.2012.01.002](https://doi.org/10.1016/j.apcatb.2012.01.002)

*Publication date:*  
2012

[Link back to DTU Orbit](#)

*Citation (APA):*  
Doronkin, D. E., Khan, T. S., Bligaard, T., Fogel, S., Gabrielsson, P., & Dahl, S. (2012). Sulfur poisoning and regeneration of the Ag/-Al<sub>2</sub>O<sub>3</sub> catalyst for H<sub>2</sub>-assisted SCR of NO<sub>x</sub> by ammonia. *Applied Catalysis B: Environmental*, 117-118, 49-58. <https://doi.org/10.1016/j.apcatb.2012.01.002>

---

### General rights

Copyright and moral rights for the publications made accessible in the public portal are retained by the authors and/or other copyright owners and it is a condition of accessing publications that users recognise and abide by the legal requirements associated with these rights.

- Users may download and print one copy of any publication from the public portal for the purpose of private study or research.
- You may not further distribute the material or use it for any profit-making activity or commercial gain
- You may freely distribute the URL identifying the publication in the public portal

If you believe that this document breaches copyright please contact us providing details, and we will remove access to the work immediately and investigate your claim.

# **Sulfur poisoning and regeneration of the Ag/ $\gamma$ -Al<sub>2</sub>O<sub>3</sub> catalyst for H<sub>2</sub>-assisted SCR of NO<sub>x</sub> by ammonia**

*Dmitry E. Doronkin<sup>1\*</sup>, Tuhin Suvra Khan<sup>2</sup>, Thomas Bligaard<sup>3</sup>, Sebastian Fogel<sup>1, 4</sup>, Pär Gabrielsson<sup>4</sup>, Søren Dahl<sup>1</sup>*

<sup>1</sup>Center for Individual Nanoparticle Functionality (CINF), Department of Physics, Technical University of Denmark, Fysikvej 307, 2800 Kgs. Lyngby, Denmark

<sup>2</sup>Center of Atomic-scale Materials Design (CAMD), Department of Physics, Technical University of Denmark, Fysikvej 307, 2800 Kgs. Lyngby, Denmark

<sup>3</sup>SUNCAT Center for Interface Science and Catalysis, SLAC National Accelerator Laboratory, Menlo Park, CA 94025, U.S.A.

<sup>4</sup>Haldor Topsøe A/S, Nymøllevej 55, 2800 Kgs. Lyngby, Denmark

\* Corresponding author: tel.: +45-4525-3275, e-mail: [dmdo@fysik.dtu.dk](mailto:dmdo@fysik.dtu.dk)

**Abstract.** Sulfur poisoning and regeneration mechanisms for a 2% Ag/ $\gamma$ -Al<sub>2</sub>O<sub>3</sub> catalyst for the H<sub>2</sub>-assisted selective catalytic reduction of NO<sub>x</sub> by NH<sub>3</sub> are investigated. The catalyst has medium sulfur tolerance at low temperatures, however a good capability of regeneration at 670 °C under lean conditions when H<sub>2</sub> is present. These heating conditions can easily be established during soot filter regeneration. Furthermore, two types of active sites could be identified with different regeneration capabilities, namely finely dispersed Ag and larger Ag nanoparticles. The most active sites are associated with the finely dispersed Ag. These sites are irreversibly poisoned and cannot be regenerated under driving conditions. On the other hand the larger Ag nanoparticles are reversibly poisoned by direct SO<sub>x</sub> adsorption. The interpretation of the data is supported by DFT calculations.

Keywords: Ag/Al<sub>2</sub>O<sub>3</sub>; SO<sub>2</sub>; NO<sub>x</sub> SCR; poisoning; regeneration

## 1. Introduction

Selective catalytic reduction (SCR) is the leading NO<sub>x</sub> control technique for diesel vehicles with ammonia used as a reductant. Commonly used catalysts are vanadia-based catalysts and Cu and Fe-containing zeolites. However, none of the systems demonstrate high thermal durability together with a good activity throughout the broad temperature region from 150 to 550 °C which is needed for vehicle applications [1]. Therefore, research of novel non-toxic, inexpensive and durable catalytic systems for NH<sub>3</sub>-SCR is still an important focus area.

Recently two research groups suggested to use Ag/Al<sub>2</sub>O<sub>3</sub>, which is a well-known catalyst for NO<sub>x</sub> SCR by hydrocarbons (HC-SCR), for SCR of NO<sub>x</sub> by ammonia or urea with co-feeding hydrogen, resulting in nearly 90% NO<sub>x</sub> conversion at temperatures as low as 200 °C [2,3]. Still, one of the major obstacles for the application of Ag/Al<sub>2</sub>O<sub>3</sub> for NO<sub>x</sub> SCR by ammonia is its rather poor sulfur tolerance [4]. A catalyst of 2% Ag/Al<sub>2</sub>O<sub>3</sub> demonstrated a decrease in H<sub>2</sub>-assisted NO<sub>x</sub> conversion by urea from 50% to 30% after 20 hours on stream in the presence of 50 ppm SO<sub>2</sub> at 250 °C. This is a rather good result considering the very high GHSV=380 000 h<sup>-1</sup> in the tests. However, the large amount of hydrogen (0.5%, 5:1 H<sub>2</sub>:NO) used in this study is probably unacceptable for application in diesel vehicles because such a large consumption of hydrogen leads to a high “fuel penalty” [5].

A significant amount of data on sulfur tolerance of Ag/Al<sub>2</sub>O<sub>3</sub> catalysts exists for NO<sub>x</sub> SCR by hydrocarbons. Meunier and Ross [6] observed strong deactivation of a 1.2% Ag/Al<sub>2</sub>O<sub>3</sub> catalyst for propene-SCR by 100 ppm SO<sub>2</sub> in the feed. It is noteworthy

that the authors were able to recover most of the catalyst activity by treatment in 10% H<sub>2</sub>/Ar at 650 °C or heating in the reaction mixture at 750 °C. Park and Boyer [7] compared the catalytic behavior of 2% and 8% Ag/Al<sub>2</sub>O<sub>3</sub> catalysts in the presence of SO<sub>2</sub> and concluded that high Ag loadings may be preferential for making a sulfur tolerant catalyst. The authors demonstrated prominent activation of 8% Ag/Al<sub>2</sub>O<sub>3</sub> by SO<sub>2</sub> in the feed and ascribed that to the formation of a very active silver sulfate phase.

When estimating the SO<sub>2</sub> tolerance of Ag/Al<sub>2</sub>O<sub>3</sub> catalysts attention should be given also to the process temperature. Satokawa and coworkers [8] showed a clear dependence of the propane-SCR temperature on the deactivation degree with permanent catalyst deactivation at T<500 °C and furthermore the ability to partially regenerate the catalyst by heating to 600 °C, even without removing low amounts (1 ppm) of SO<sub>2</sub> from the feed. Further studies [8] of sulfation-regeneration mechanisms included obtaining SO<sub>2</sub> TPD profiles and attribution of peaks to different types of adsorbed SO<sub>2</sub>, bound to Ag and alumina. The catalyst regeneration temperature was lower than any of the SO<sub>2</sub> desorption peaks, observed in the study, which did not allow drawing a clear conclusion about the deactivation and regeneration mechanisms.

Breen with coworkers [9] also demonstrated a drastic dependence of the catalyst degree of poisoning on the temperature of NO<sub>x</sub> SCR by octane and toluene. The following was observed; at low temperatures (<235 °C) little deactivation, between 235 and 500 °C – severe deactivation and at T>590 °C – activation due to a suppression of unselective oxidation of hydrocarbons. The low temperature sulfur tolerance was ascribed to low catalyst activity in SO<sub>2</sub> oxidation to SO<sub>3</sub> with the latter considered to be the main poisoning agent for Ag/Al<sub>2</sub>O<sub>3</sub>. The authors have evaluated a few regeneration options of which heating to 650 °C in hydrogen-containing lean mixture showed

promising results rather than regeneration under oxidizing conditions without H<sub>2</sub>. The fastest regeneration technique included heating the catalyst a rich mixture containing CO and hydrogen.

The results of other research groups [10, 11] agree with Breen's results in SO<sub>2</sub> oxidation to SO<sub>3</sub> by NO<sub>2</sub> being the major step in the sulfur poisoning of Ag/Al<sub>2</sub>O<sub>3</sub> catalysts. Partial regeneration of the catalyst was observed after heating to 600 °C in a hydrocarbon-containing feed.

In this work we have attempted to reveal the Ag/Al<sub>2</sub>O<sub>3</sub> sulfation and regeneration mechanisms, which will allow us to develop an efficient regeneration strategy for the ammonia SCR catalyst in question. Special attention was given to the catalyst operation below 300 °C for applications in light-duty diesel vehicles low temperatures are of great importance [10]. The suggested mechanism was supported by DFT calculations. The regeneration strategy using the high temperatures developed during Diesel Particulate Filter (DPF) regeneration in diesel cars was evaluated.

## **2. Experimental**

### *2.1. Catalyst preparation*

Parent  $\gamma$ -alumina (Puralox TH 100/150, S<sub>BET</sub> = 150 m<sup>2</sup>/g) was kindly provided by SASOL. 1-3 wt.% Ag/Al<sub>2</sub>O<sub>3</sub> were obtained by incipient wetness impregnation of parent  $\gamma$ -alumina by AgNO<sub>3</sub> (Sigma-Aldrich) dissolved in deionized water. After impregnation the catalyst was dried at room temperature overnight and calcined at 550 °C for 4 hours in static air. The calcined catalyst was tableted, crushed and sieved to obtain a 0.18 – 0.35 mm fraction (mesh 80 – mesh 45) used in the catalytic tests. A new batch of catalyst was sulfated and used to test every new regeneration recipe.

## *2.2. Determination of the specific surface area*

The specific surface areas ( $S_{\text{BET}}$ ) of the catalysts were measured by  $\text{N}_2$ -adsorption with a Micromeritics Gemini instrument. Untreated catalysts were measured in powder form and for the catalysts after testing a 0.18 – 0.35 mm fraction of particles (as in catalytic tests) was used for the BET measurement.

## *2.3. Catalysis*

Temperature-programmed activity tests were carried out in a fixed-bed flow reactor (quartz tube with 4 mm inner diameter) in a temperature programmed mode while the temperature was decreased from 400 °C to 150 °C with a rate of 2 °C/min. Prior to the temperature ramp the catalyst was heated to 470 °C for 30 min. in the gas mixture used for the tests. The temperature was controlled using a Eurotherm 2408 temperature controller with a K-type thermocouple. 45 mg of catalyst was diluted with 100 mg of SiC (mesh 60) and placed on a quartz wool bed. The bed height was ~11 mm and the GHSV, calculated using the volume of the pure catalyst was  $\sim 110\,000\text{ h}^{-1}$ . The gas composition normally contained 500 ppm NO, 520 ppm  $\text{NH}_3$ , 1200 ppm of  $\text{H}_2$ , 8.3%  $\text{O}_2$ , and 7% water balanced with Ar. For sulfur poisoning tests 10 ppm  $\text{SO}_2$  was admixed to the feed. Water was dosed by an ISCO 100DM syringe pump through a heated capillary. Reaction products were analyzed by a Thermo Fisher Nicolet 6700 FTIR analyzer, equipped with a 2 m gas cell. Gas capillaries were heated to  $\sim 130\text{ }^\circ\text{C}$  and the FTIR gas cell to 165 °C to avoid condensation of water and formation of ammonium nitrate.

Conversions were calculated using the following equations:

$$X_{NO_x} = 1 - \frac{C_{NO_x}^{outlet}}{C_{NO_x}^{inlet}}, \quad (1)$$

$$\text{and } X_{NH_3} = 1 - \frac{C_{NH_3}^{outlet}}{C_{NH_3}^{inlet}}, \quad (2)$$

where  $X_{NO_x}$  denotes the conversion of  $NO_x$  to  $N_2$  and  $C_{NO_x}^{inlet}$  and  $C_{NO_x}^{outlet}$  is the  $NO_x$  concentrations at the inlet and outlet of the reactor respectively, where:

$$C_{NO_x} = C_{NO} + C_{NO_2} + C_{N_2O}. \quad (3)$$

#### 2.4. DFT calculations

The plane wave density functional theory (DFT) code DACAPO was used to calculate the adsorption energies and the gas phase energies of the adsorbates [12]. A plane wave cutoff of 340.15 eV and a density cutoff of 680 eV was used in the calculations. The core electrons were described by Vanderbilt ultrasoft pseudopotentials. The RBPE functional was used for describing the exchange correlation energy [13].

The adsorption energies of the  $SO_2$ ,  $SO_3$ , and  $SO_4$  species were studied over the Ag (111) terrace and (211) step surfaces, on a  $\gamma$ - $Al_2O_3$  model step surface, and two single Ag sites constructed by replacing one Al atom for Ag in the alumina step surface and by attaching one Ag atom to the  $\gamma$ - $Al_2O_3$  step (see supplementary material for the geometries).

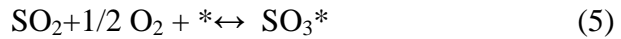
For the Ag (111) and (211) surfaces, we used a  $4 \times 4 \times 1$  Monkhorst-Pack  $\mathbf{k}$ -point sampling in the irreducible Brillouin zone. We employed a  $3 \times 3$  surface cell for the Ag (111) and  $3 \times 1$  surface cell for the Ag (211) surfaces. For the (111) surface we used a four-layer slab where the two top-most layers were allowed to relax, whereas for the

(211) surfaces we used a slab model with nine layers and the topmost three layers are allowed to relax. In all the model calculations, neighboring slabs were separated by more than 10 Å of vacuum.

For the calculation of  $\gamma$ -Al<sub>2</sub>O<sub>3</sub> and the adsorption of different species on  $\gamma$ -Al<sub>2</sub>O<sub>3</sub> we also used the DACAPO code with a plane wave cutoff of 340.15 eV and a density cutoff of 680 eV. A  $4 \times 4 \times 1$  Monkhorst-Pack **k**-point sampling in the irreducible Brillouin zone was used for  $\gamma$ -Al<sub>2</sub>O<sub>3</sub>. The  $\gamma$ -Al<sub>2</sub>O<sub>3</sub> surface was modeled by a step on a nonspinel  $\gamma$ -Al<sub>2</sub>O<sub>3</sub> structure which was derived from bulk  $\gamma$ -Al<sub>2</sub>O<sub>3</sub> model in [14]. The cell parameters for the  $\gamma$ -Al<sub>2</sub>O<sub>3</sub> model step surface are  $a = 8.0680$  Å and  $b = 10.0092$  Å and  $\alpha = \beta = \gamma = 90^\circ$ . For the  $\gamma$ -Al<sub>2</sub>O<sub>3</sub> surface the bottom two layers were fixed whereas the top-most three layers were allowed to relax. In all the model  $\gamma$ -Al<sub>2</sub>O<sub>3</sub> surfaces, the neighboring slabs are separated by more than 10 Å of vacuum.

SO<sub>x</sub> adsorption energies were calculated relative to gas phase energies of SO<sub>2</sub>(g) + O<sub>2</sub>(g).

In the case of the Ag (111) and Ag (211) surfaces desorption of SO<sub>4</sub> as the most stable species was considered as SO<sub>2</sub>(g) + O<sub>2</sub>(g). For calculation of desorption temperatures for SO<sub>2</sub> and SO<sub>3</sub> we used the following procedure. Starting from the chemical equation:



where \* is the free surface site and SO<sub>x</sub>\* is the adsorbed species. We can write down the ratio of occupied and free adsorption sites:

$$\frac{\theta_{\text{SO}_x}}{\theta^*} = K_{\text{ads}} \cdot P_{\text{SO}_x} = \exp\left(-\frac{\Delta G_{\text{ads}}}{kT}\right) \cdot P_{\text{SO}_x} = \exp\left(\frac{-(\Delta G_{\text{ads}}^\ominus - kT \ln P_{\text{SO}_x})}{kT}\right) \quad (6)$$



that at the desorption temperature the numbers of occupied and free adsorption sites will equal ( $\Theta_{SO_x} = \Theta^*$ ), which gives:

$$\Delta G_{ads}^{\ominus} - kT \ln P_{SO_x} = 0, \text{ or} \quad (7)$$

$$\Delta E_{ads} - \Delta ZPE_{ads} - T \cdot \Delta S_{ads} - kT \ln P_{SO_x} = 0, \quad (8)$$

We calculate the ZPE (zero point energy) and the entropy of the  $SO_x$  in their adsorbed state and so it is possible to calculate the desorption temperature for a given partial pressure of  $SO_x$ :

$$T = \frac{\Delta E_{ads}}{k \ln P_{SO_x} - \Delta S_{gas}}. \quad (9)$$

The  $SO_x$  entropy and ZPE found for  $\gamma\text{-Al}_2\text{O}_3$  model surface were used for the single Ag atom sites on the  $\gamma\text{-Al}_2\text{O}_3$ . Standard entropy values for  $SO_2$  and  $SO_3$  from [15] (neglecting entropy change with temperature) and a partial pressure of  $SO_x$   $4 \cdot 10^{-7}$  bar (0.4 ppm in [9]) and partial pressure of  $O_2$  is 0.07 bar [9] were used in the calculations.

### 3. Results and discussion

#### 3.1. Catalyst choice: stability of Ag/ $Al_2O_3$ and options for the regeneration

##### 3.1.1. The catalyst choice

Temperature dependence of  $NO_x$  and  $NH_3$  conversions for the fresh 1-3% Ag/ $Al_2O_3$  catalysts is shown on figures 1a and 1b respectively. 1% Ag/ $Al_2O_3$  exhibits SCR onset at 130 °C reaching 80%  $NO_x$  conversion at 200 °C and leveling  $NO_x$  conversion at 90% at  $T > 300$  °C. This is in agreement with previous studies [2]. 2% and 3% Ag/ $Al_2O_3$  catalysts demonstrate SCR onset shifted by 7 °C to lower temperatures compared 1%, but lower maximum conversion and generally lower SCR activity at higher temperatures, unlike results of Shimizu and Satsuma [3]. The  $NH_3$  conversion follow

the  $\text{NO}_x$  conversion at  $T < 270\text{--}300\text{ }^\circ\text{C}$ . At higher temperature  $\text{NH}_3$  becomes oxidized and the  $\text{NH}_3$  conversion is higher than  $\text{NO}_x$  conversion. Thus,  $\text{NH}_3$  oxidation plays some role in the decrease of high temperature  $\text{NO}_x$  conversion but this is not the main reason. The reason for observing conversion maxima for 2% and 3%  $\text{Ag}/\text{Al}_2\text{O}_3$  catalysts at  $200\text{ }^\circ\text{C}$  with subsequent drop in  $\text{NH}_3$  and  $\text{NO}_x$  conversions could be direct oxidation of  $\text{H}_2$  by oxygen taking over. As it was shown earlier no  $\text{NO}$  and  $\text{NH}_3$  is converted over an  $\text{Ag}/\text{Al}_2\text{O}_3$  catalyst in the absence of  $\text{H}_2$  [16]. Another possible reason is the lack of strong acid sites for  $\text{NH}_3$  adsorption in the 2-3%  $\text{Ag}/\text{Al}_2\text{O}_3$  catalysts which is demonstrated in [17].

Noteworthy, the tested catalysts demonstrate very high stability at temperature up to  $700\text{ }^\circ\text{C}$  which has also been shown in the number of papers on HC-SCR [3, 9]. To further check the thermal stability of the 1%  $\text{Ag}/\text{Al}_2\text{O}_3$  catalyst it was subjected to hydrothermal deactivation at  $750\text{ }^\circ\text{C}$  for 16 hours. The activity of the obtained catalyst is reported in figs. 1a and 1b as gray dotted lines. The low-temperature conversion is only slightly shifted by  $3\text{ }^\circ\text{C}$ , whereas at  $T > 300\text{ }^\circ\text{C}$  one may observe a decrease in  $\text{NO}_x$  and  $\text{NH}_3$  conversions similar to that observed for catalysts with higher Ag loading. This may indicate sintering of Ag particles leading to the increased unselective oxidation of hydrogen. At the same time, the relatively small decrease of the catalyst specific surface area ( $S_{\text{BET}}$ ) does not indicate any significant change in the alumina support (table 1).

Contrary to the hydrothermal aging, sulfur poisoning of  $\text{Ag}/\text{Al}_2\text{O}_3$  leads to significant catalyst deactivation. Preliminary experiments on the choice of sulfur poisoning temperature showed no catalyst deactivation with  $\text{SO}_2$  in the feed at  $500\text{ }^\circ\text{C}$  and the most severe deactivation in the temperature range  $200\text{--}300\text{ }^\circ\text{C}$  in very good agreement with the earlier reported results for HC-SCR [8, 9]. Therefore, preliminary

SO<sub>2</sub> deactivation studies of 1-3%Ag/Al<sub>2</sub>O<sub>3</sub> were performed at 200-227 °C and all the following deactivation-regeneration studies of 2%Ag/Al<sub>2</sub>O<sub>3</sub> were done at 250 °C (Fig. 1c). For the comparison of regeneration methods the SO<sub>2</sub> poisoning was obtained by introducing 10 ppm SO<sub>2</sub> to the SCR feed for 4 hours.

Catalytic performance of 1-3%Ag/Al<sub>2</sub>O<sub>3</sub> in NO<sub>x</sub> SCR after such sulfur treatment at 200-227 °C is shown on fig. 1d. Lowering deactivation temperature from 250 °C to 200 °C leads to a very small shift of the low-temperature activity within 5 °C, therefore, the temperature difference is not the determining factor for the observed activity difference. 1%Ag/Al<sub>2</sub>O<sub>3</sub> was poisoned to the highest degree, whereas higher Ag loading led to better sulfur tolerance with 3%Ag/Al<sub>2</sub>O<sub>3</sub> showing the highest NO<sub>x</sub> conversion at T < 300 °C. It should be noted that after exposure to SO<sub>2</sub> (and even after regeneration of 1% and 2%Ag/Al<sub>2</sub>O<sub>3</sub> catalysts at 670 °C) the NH<sub>3</sub> conversion profiles coincided with the NO<sub>x</sub> conversion profiles for all tested samples. That indicates quenching of NH<sub>3</sub> unselective oxidation over 1-3%Ag/Al<sub>2</sub>O<sub>3</sub> by SO<sub>2</sub>. Due to the similarity of NO<sub>x</sub> and NH<sub>3</sub> conversion curves for the sulfated catalysts only NO<sub>x</sub> conversions will be reported throughout the article.

Sulfation of 2 and 3%Ag/Al<sub>2</sub>O<sub>3</sub> leads not only to a shift of the maximum NO<sub>x</sub> conversion to higher temperatures but also to an increase to significantly higher values than demonstrated over the fresh catalysts. The shift of the maximum activity of 2%Ag/Al<sub>2</sub>O<sub>3</sub> along with “activation” of the catalyst at 227 °C (near the conversion maximum of the fresh catalyst) and at 250 °C can be seen in Fig. 1c. Higher SO<sub>2</sub> exposure leads to a shift of the maximum NO<sub>x</sub> conversion to higher temperatures along with deterioration of the low-temperature activity. The activity gain induced by sulfation has been observed earlier and attributed to the redistribution of Ag species [4].

However, as we have observed the decrease of unselective  $\text{NH}_3$  oxidation after  $\text{SO}_2$  exposure, we suppose the  $\text{SO}_x$  blocking of sites active in  $\text{NH}_3$  and  $\text{H}_2$  oxidation to play a major role in the increased  $\text{NO}_x$  conversion over 2 and 3%  $\text{Ag}/\text{Al}_2\text{O}_3$  catalysts. At the same time  $\text{SO}_2$  adsorption increases the alumina acidity which can also play the role for the SCR activity as discussed in a separate publication [17].

Several options for the catalyst regeneration under hydrocarbon (HC) SCR have been suggested in the literature. All of them include heating sulfated  $\text{Ag}/\text{Al}_2\text{O}_3$  in different media – oxidizing [9], hydrogen (or hydrocarbon)-containing lean exhaust [6, 8, 9, 10] or rich exhaust [6, 9].

Heating sulfated 2%  $\text{Ag}/\text{Al}_2\text{O}_3$  to 670 °C for 10 min in the  $\text{NO}_x$  SCR feed without hydrogen leads only to a small 10 °C shift of T50% to lower temperatures (not shown). Therefore, regeneration of  $\text{Ag}/\text{Al}_2\text{O}_3$  for  $\text{NO}_x$  SCR by  $\text{NH}_3$  without co-feeding hydrogen is ineffective. Thus, regeneration at 670 °C in the reaction gas mixture was used to test the regeneration capability of 1-3%  $\text{Ag}/\text{Al}_2\text{O}_3$  catalysts. Activity of the catalysts regenerated during 40 min. is reported in fig. 1e. All catalysts partially regained the low-temperature activity, however, the high-temperature activity of 3%  $\text{Ag}/\text{Al}_2\text{O}_3$  was decreased compared to the sulfated catalyst. At the same point this catalyst demonstrated a higher conversion of  $\text{NH}_3$  compared to  $\text{NO}_x$  at  $T > 350$  °C, indicating  $\text{NH}_3$  oxidation. 2%  $\text{Ag}/\text{Al}_2\text{O}_3$  showed the highest  $\text{NO}_x$  conversion throughout the whole temperature region and will therefore, be used for the further study. For the simplicity in the text below and the following figures 2%  $\text{Ag}/\text{Al}_2\text{O}_3$  will be referred as  $\text{Ag}/\text{Al}_2\text{O}_3$ .

### *3.1.2. Regeneration options*

To simulate regeneration in rich exhaust the catalyst was heated to 670 °C for 1 min. with oxygen removed from the feed. The activity following from this rich regeneration is presented on fig. 2a as a solid line. The profile is significantly shifted to lower temperatures compared to the non-regenerated sample. Another feature is the maximum NO<sub>x</sub> conversion (96%), which is now higher than that of both the fresh and the non-regenerated catalysts. Still, regeneration under rich conditions did not allow to regain the low-temperature activity completely.

However, obtaining rich exhaust from diesel engine leads to high fuel consumption and is, therefore, undesirable. Thus, we have preferred relatively fast catalyst regeneration under lean conditions with co-feeding hydrogen. The NO<sub>x</sub> conversion profile for Ag/Al<sub>2</sub>O<sub>3</sub> regenerated 10 min. at 670 °C in the standard NO<sub>x</sub> SCR feed (with hydrogen) is shown on fig. 2a as a dashed line. The catalyst shows the same activity below 200 °C as when regenerated under rich conditions and at higher temperatures even higher conversion (up to 100%). At the same time the surface area of the catalyst regenerated for 10 minutes is not deteriorated compared to the fresh catalyst (table 1). This kind of regeneration is very easy to implement in diesel vehicles because it can coincide with regeneration of the DPF, which requires a similar heating strategy.

### *3.2. Influence of the regeneration time on the catalyst activity*

Regeneration time is of high importance for automotive catalysts, as heating the catalyst requires a lot of energy, i.e. fuel to be spent. Influence of the regeneration time (for regeneration under lean conditions with co-feeding hydrogen) on the activity of the regenerated catalyst is shown in fig. 2b. The value on the Y-axis is the shift of

temperature for 50% NO<sub>x</sub> conversion over the regenerated catalyst relative to the fresh catalyst :

$$T_{50\% \text{ shift}} = T_{50\%}^{\text{regenerated}} - T_{50\%}^{\text{fresh}}. \quad (10)$$

Zero at the timescale stands for non-regenerated catalyst. Heating to 670 °C for 1 min. leads to the shift of T 50% by 24 °C towards lower temperatures, which is already very good. Heating for 10 min. allows us to get 6 °C lower T 50%, but further treatment at high temperatures does not lead to significant further activation of the catalyst. The best T 50%, we could get by regenerating Ag/Al<sub>2</sub>O<sub>3</sub>, is 15 °C higher than T 50% of the fresh Ag/Al<sub>2</sub>O<sub>3</sub>. That result is obtained after 40 min of regeneration. Higher regeneration time does not yield better activity but causes loss of the catalyst surface area (table 1) and is, therefore, undesirable. It is worth noting that we were not able to match the low-temperature activity of the fresh catalyst after regeneration.

### *3.3. Developing a deactivation – regeneration strategy to mimic automotive catalyst operating conditions*

Typical lifecycle of an automotive light-duty Ag/Al<sub>2</sub>O<sub>3</sub> NO<sub>x</sub> SCR catalyst comprises normal driving, during which the catalyst operates at low temperatures 150 – 350 °C [10] and is poisoned by sulfur, and regeneration which optimally coincides with regeneration of the DPF. To be more precise, useful vehicle running time according to the modern Euro 5 and Euro 6 standards is 160 000 km [18], and typical intervals between DPF regenerations are 300 to 900 km (with the modern Volvo D5 light-duty diesel engine as an example ) [19], which gives a minimum of 160 catalyst regeneration cycles. Using average fuel consumption of this engine during urban driving (6.7 l/100 km with a manual gearbox), an average diesel fuel density approx. 850 g/l [20], and a

maximum allowed sulfur content of 10 ppm in the diesel fuel [21], the total sulfur passed through the catalyst will amount to 91 g or 2.85 mol. Using available data on the volume of monolith catalyst for the mentioned engine (9 liters) and the monolith density 2.5 g/in<sup>3</sup> [10], the weight of the washcoat for an automotive catalyst (15% of the total) and the relative weight of the powder catalyst in the washcoat (80%) [22] we get a total of 0.47 g (14.7 mmol) sulfur per gram of powder catalyst during the vehicle lifetime. Therefore, the amount of sulfur per one deactivation cycle will be 83  $\mu$ mol per gram of catalyst, assuming adsorption of all sulfur. In reality, however, not all sulfur will be adsorbed partly due to very high or low temperatures [9].

In our tests we have chosen the scheme involving catalyst poisoning with 10 ppm SO<sub>2</sub> at intermediate temperature of 250 °C for 1 hour which gives us a sulfur exposure before regeneration of 65  $\mu$ mol per gram of catalyst, which is close to the theoretical maximum value calculated above. Thus, we will use this protocol as "worst case" scenario.

Figs. 3a and Figs. 3b show two different ways of testing sulfur tolerance with the same total sulfur exposure (4 hours with 10 ppm SO<sub>2</sub>, corresponds to 260  $\mu$ mol/g catalyst) and the same regeneration time, but split by four relatively small regeneration segments in the second case.

The comparison of the catalyst activity after these two tests is given on fig. 3c. Evidently, the low-temperature activities of the two poisoned catalysts are identical. The data in Figs. 3a and 3b does not allow us to state that the regenerated catalyst activity observed in fig. 3c represents "steady state" automotive catalyst activity in both cases. Further testing is needed to reveal "steady state" catalyst activity during sulfation – regeneration cycles.

### *3.4. Cycling deactivation – regeneration*

In order to clarify if the catalyst will be further deactivated after many 1 h. SO<sub>2</sub> poisoning – 10 min. regeneration cycles we have carried out 30 deactivation (at 250 °C) – regeneration (at 670 °C) cycles. Evolution of the NO<sub>x</sub> and NH<sub>3</sub> conversions during the first 9 cycles of the experiment is shown in fig. 4.

During the sulfation of the fresh catalyst (first 60 min.) NO<sub>x</sub> conversion steadily increases. During heating the catalyst to 670 °C the NO<sub>x</sub> conversion drops to slightly negative values. According to eq. (1) in the section 2.3 this is due to a higher NO<sub>x</sub> concentration at the reactor outlet than at the inlet. The latter is caused by oxidation of part of ammonia to NO<sub>x</sub> at the regeneration temperature which can be seen by the higher conversion of NH<sub>3</sub> compared to NO<sub>x</sub> at T>500 °C. To prevent ammonia oxidation in the real life application it is possible to switch off ammonia supply during regeneration without compromising regeneration efficiency.

The NO<sub>x</sub> conversion following regeneration is maximal (97%) after the first regeneration and decreases only a little (to 95%) with further regeneration cycles. However, sulfur poisoning of the regenerated sample leads to a decrease in the NO<sub>x</sub> conversion at the end of each of the first deactivation cycles. This decrease in NO<sub>x</sub> conversion could indicate that during each of these first regenerations the SO<sub>x</sub> adsorbed during the preceding deactivation cycle is not completely removed from the catalyst surface. After seven sulfation-regeneration cycles NO<sub>x</sub> conversion is stabilized, so each new testing cycle yields the same profile as the previous. Thus, further sulfation and regeneration do not change the catalyst performance.



Integration of the SO<sub>2</sub> signal measured by FTIR during 10<sup>th</sup> – 20<sup>th</sup> cycles (they are all equal) gives the amount of SO<sub>2</sub> equal to the amount of SO<sub>2</sub> passed through the catalyst during these cycles. Therefore, using FTIR data we can estimate the amount of SO<sub>2</sub>, which was accumulated in the catalyst and not desorbed during the first regenerations to be 0.11 mmol per gram catalyst.

Our data (not shown) suggests that the SO<sub>2</sub> poisoning effect is cumulative in the range of SO<sub>2</sub> concentrations 0.5 – 10 ppm, i.e. the catalyst deactivation degree depends only on total SO<sub>2</sub> exposure. Therefore, with the same SO<sub>x</sub> exposure between DPF regenerations as in this study real catalyst performance will be high enough even in the end of a sulfation cycle before the next regeneration.

### *3.5. Mechanism of Ag/Al<sub>2</sub>O<sub>3</sub> sulfation and regeneration*

The results obtained in the previous section 3.4. set the ground for a few conclusions regarding the sulfation and regeneration mechanisms for Ag/Al<sub>2</sub>O<sub>3</sub> catalysts of hydrogen-assisted NO<sub>x</sub> SCR by NH<sub>3</sub>.

First of all, some amount of SO<sub>x</sub> is not desorbed after regeneration. This amount was estimated in the previous section and is reproducible. At the same time we cannot regenerate the full low-temperature activity of Ag/Al<sub>2</sub>O<sub>3</sub>, no matter if lean hydrogen-containing or rich mixtures were used for the regeneration. The SCR reaction onset for the sulfated and regenerated catalyst is always shifted to higher temperatures. Therefore, we suppose that a certain type of active sites exists (name it “Type I”), which stand for Ag/Al<sub>2</sub>O<sub>3</sub> activity at low temperatures (<200 °C), that are irreversibly poisoned by SO<sub>2</sub> and can not be regenerated using standard techniques. Taking into account the very low

sulfur tolerance of low-loaded Ag/Al<sub>2</sub>O<sub>3</sub> [6,7], we can attribute Type I active sites to highly dispersed silver e.g. Ag<sup>δ+</sup> atoms or Ag<sup>+</sup> ions [23, 24] (see Fig. 5).

SO<sub>x</sub> adsorption on the alumina surface (where dispersed silver is localized) blocks these type I active sites. SO<sub>x</sub> can be adsorbed on single-atom Ag sites on the alumina as well as on the neighboring Al atoms. It is impossible to desorb SO<sub>x</sub> from the alumina surface by heating the catalyst to 670 °C [25] and, therefore, Type I active sites could not be regenerated.

Another evidence of irreversibly poisoned active sites is the formation of excess of nitrogen dioxide over the fresh catalyst (fig. 6b, solid line), a catalytic function which is irreversibly poisoned by SO<sub>2</sub> and cannot be regenerated (fig. 6b, dotted line). Therefore, we also attribute the increased NO oxidation capacity to Type I active sites.

However, the possibility of regeneration of the most of the SCR activity of Ag/Al<sub>2</sub>O<sub>3</sub> hints on the existence of “Type II” active sites. As they are more abundant in more SO<sub>2</sub> tolerant high-loaded Ag/Al<sub>2</sub>O<sub>3</sub> [7] we attribute them to the surface of Ag nanoparticles. It has been shown that it is possible to desorb SO<sub>2</sub> from the Ag surface at temperatures near 600 °C [25]. Thus, we assume that sulfation and regeneration of these Type II active sites determines the SCR activity of Ag/Al<sub>2</sub>O<sub>3</sub> with sulfur-containing fuel in diesel vehicles. According to the SCR mechanism suggested in [16] these type II species are also capable of oxidizing NO to NO<sub>2</sub> which further reacts with NH<sub>3</sub> over alumina. However, type II sites are less active which leads to the deficit of NO<sub>2</sub> and prevents observing it in the gas phase when NH<sub>3</sub> is present.

Our assumption about the existence and function of Type I active sites can be verified by the following. As follows from the SO<sub>2</sub> TPD profiles in [11, 25] it is possible to desorb SO<sub>x</sub> from alumina surface at ca. 1000 °C. Of course, the alumina will

undergo partial restructuring at this temperature [26] accompanied by the formation of the  $\alpha$ - $\text{Al}_2\text{O}_3$  phase, which will partially ruin the catalyst. However, this may help to test the principle.

The results of heating of sulfated  $\text{Ag}/\text{Al}_2\text{O}_3$  to 950 °C in the SCR gas mixture with further immediate cooling are shown in figs. 6a and 6b as dashed lines. By removing  $\text{SO}_x$  from the alumina surface (observed by FTIR) we were able to regain SCR onset at the same temperature as for the fresh  $\text{Ag}/\text{Al}_2\text{O}_3$  (fig. 6a). At the same time we were able to regenerate excessive  $\text{NO}_2$  production (fig. 6b) which was impossible to get by any kind of regeneration at lower temperature. Still, the maximum activity of the catalyst was lower than that of the fresh catalyst resembling the activity of 3% $\text{Ag}/\text{Al}_2\text{O}_3$  (fig. 1a). The specific surface area of the catalyst regenerated at 950 °C did not change significantly compared to the fresh sample (table 1), therefore, it is rather sintering of Ag particles which caused a drop in the maximum activity. Thus, we consider possibility of regenerating low temperature activity as an evidence for the existence of several types of active sites in  $\text{Ag}/\text{Al}_2\text{O}_3$  as was previously stated for HC-SCR  $\text{Ag}/\text{Al}_2\text{O}_3$  catalysts [27].

The fact that  $\text{SO}_x$  irreversibly adsorbed on the alumina surface does not hinder that the SCR reaction can be explained if we assume that Ag species participate in the oxidation of NO to  $\text{NO}_2$  and the alumina facilitates further reaction of NO,  $\text{NO}_2$  and  $\text{NH}_3$  according to the “Fast SCR” mechanism [28]. Since “Fast SCR” occurs over a number of acidic surfaces, sulfated alumina should catalyze SCR as well if  $\text{SO}_x$ -free Ag surface is left to oxidize NO.

### *3.6. Evaluation of the proposed sulfation and regeneration mechanism of Ag/Al<sub>2</sub>O<sub>3</sub> by DFT*

Adsorption energies of SO<sub>2</sub>, SO<sub>3</sub>, and SO<sub>4</sub> for the most energetically favorable adsorption geometries for different adsorption sites are summarized in the Table 2 and the corresponding geometries for the  $\gamma$ -alumina model step surface are shown in Fig. 7. It should be noted that SO<sub>x</sub> can be adsorbed on the  $\gamma$ -alumina in different configurations with similar energies and only the lowest energies (strongest adsorption) are shown. The DFT calculation shows that the SO<sub>x</sub> adsorbs strongly on the step sites which is expected from the low coordination of these sites and the steric freedom available at the step sites [29 - 31]. At the same time the surface step is representative of small 1-3 nm nanoparticles containing mostly undercoordinated surface atoms [32].

Two trends can be identified from these values. First global trend is that all types of SO<sub>x</sub> bind significantly stronger to the alumina surface than the metal surface. The adsorption sites also include single Ag sites at the alumina surface with Ag atom built in the surface substituting Al is binding SO<sub>x</sub> most strongly. This can be explained by a thermodynamically unfavorable defect structure of this site. Secondly, the oxidation of SO<sub>2</sub> to SO<sub>3</sub> is thermodynamically favorable, with subsequent poisoning of the catalyst surface by the resulting SO<sub>3</sub>. This has been suggested in [9] and probably involves reaction with NO<sub>2</sub> [11]. SO<sub>2</sub> alone cannot be adsorbed on the studied metallic Ag surfaces under reaction conditions and SO<sub>x</sub> can, thus, only poison the alumina support or single Ag sites on this surface.

The calculated desorption temperatures (table 2) are low but the order, at which regeneration of Type II (Ag surface) and Type I (highly dispersed Ag on the alumina) occurs is in agreement with the mechanism of Ag/Al<sub>2</sub>O<sub>3</sub> poisoning and regeneration

suggested in the section 3.5. The difference between calculated and experimental desorption temperatures [11, 25] might indicate the formation of bulk silver sulfate [7, 33, 34].

At the same time addition of hydrogen significantly enhances catalyst regeneration i.e. removal of  $\text{SO}_x$  which could be due to the formation of the correspondent  $\text{HSO}_x$  species with their subsequent desorption. Table 3 shows the energies of the  $\text{HSO}_x$  species in the gas phase and adsorbed on the most energetically favorable sites. The corresponding adsorption energies are calculated as a difference between the energy in the adsorbed state and gas phase energy. According to the given numbers, the formation of  $\text{HSO}_4$  and  $\text{H}_2\text{SO}_4$  species is highly favorable on all modeled adsorption sites and as the adsorption energies of  $\text{HSO}_4$  and  $\text{H}_2\text{SO}_4$  with respect to  $\text{H}_2\text{SO}_4$  (g) is very small (-0.17 eV for  $\text{HSO}_4$  desorbing as  $\text{H}_2\text{SO}_4$  from Ag (211) and -0.28 eV for  $\text{H}_2\text{SO}_4$  on the  $\gamma$ - $\text{Al}_2\text{O}_3$  step surface) it can be easily desorbed from the catalytic surface. Thus, presence of  $\text{H}_2$  may promote the desorption of  $\text{SO}_x$  species from the catalyst surface via formation of  $\text{H}_2\text{SO}_4$  (g) in agreement with the experimental observations.

#### **4. Conclusions**

Sulfur tolerance and regeneration options of 2% Ag/ $\gamma$ - $\text{Al}_2\text{O}_3$  catalyst for  $\text{H}_2$ -assisted  $\text{NO}_x$  SCR by  $\text{NH}_3$  have been tested. The catalyst has medium sulfur tolerance at low temperatures, however a good capability of regeneration. This regeneration should include heating to 650 – 700 °C for 10 – 20 min., provided the SCR gas feed is unchanged (ammonia may be removed) and hydrogen is co-fed. Regeneration of Ag/ $\text{Al}_2\text{O}_3$  without oxygen (rich mixture) leads to essentially the same effect, but requires less time.

Heating to 650 – 700 °C does not allow full regeneration of low-temperature activity and does not allow recovery of NO<sub>2</sub> formation over Ag/Al<sub>2</sub>O<sub>3</sub> in the course of SCR.

During the long-term tests with cycling poisoning – regeneration periods catalyst activity is regenerated during each regeneration cycle, but at least for the first 6-7 cycles sulfur species are accumulated on the catalyst. Presumably, SO<sub>x</sub> is removed from Ag, but not from the alumina surface during standard regeneration, which allows us to make a conclusion on the existence of different active sites in Ag/Al<sub>2</sub>O<sub>3</sub>, namely finely dispersed Ag ions and Ag nanoparticles.

## **5. Acknowledgements**

This work was supported by The Danish Council for Strategic Research through grant 09-067233.

## References

- [1] T.V. Johnson, *Int. J. Engine Res.* 10 (2009) 275-285
- [2] M. Richter, R. Fricke, and R. Eckelt, *Catal. Lett.* 94 (2004) 115-118
- [3] K.-I. Shimizu and A. Satsuma, *Appl. Catal. B* 77 (2007) 202-205
- [4] A. Abe, N. Aoyama, S. Sumiya, N. Kakuta, and K. Yoshida, *Catal. Lett.* 51(1998) 5-9
- [5] H. Kannisto, X. Karatzas, J. Edvardsson, L.J. Pettersson, and H.H. Ingelsten, *Appl. Catal. B* 104 (2011) 74-83
- [6] F.C. Meunier and J.R.H. Ross, *Appl. Catal. B* 24 (2000) 23–32
- [7] P.W. Park and C.L. Boyer, *Appl. Catal. B* 59 (2005) 27–34
- [8] S. Satokawa, K.-I. Yamaseki, and H. Uchida, *Appl. Catal. B* 34 (2001) 299-306
- [9] J.P. Breen, R. Burch, C. Hardacre, C.J. Hill, B. Krutzsch, B. Bandl-Konrad, E. Jobson, L. Cider, P.G. Blakeman, L.J. Peace, M.V. Twigg, M. Preis, and M. Gottschling, *Appl. Catal. B* 70 (2007) 36–44
- [10] F. Klingstedt, K. Eränen, L.-E. Lindfors, S. Andersson, L. Cider, C. Landberg, E. Jobson, L. Eriksson, T. Ilkenhans, and D. Webster, *Top. Catal.* 30/31 (2004) 27-30
- [11] Q. Ma, Y. Liu, and H. He, *J. Phys. Chem. A* 112 (2008) 6630–6635
- [12] B. Hammer, L.B. Hansen, and J.K. Nørskov, *Phys. Rev. B* 59 (1999) 7413–7421
- [13] E. Mènendez-Proupin and G. Gutiérrez, *Phys. Rev. B* 72 (2005) 35116-35119
- [14] M. Digne, P. Sautet, P. Raybaud, P. Euzen, and H. Toulhoat, *J. Catal.*, 226 (2004) 54–68
- [15] Chase, M.W. Jr., *NIST-JANAF Thermochemical Tables, Fourth Edition*, *J. Phys. Chem. Ref. Data*, Monograph 9, 1998, 1-1951
- [16] D.E. Doronkin, S. Fogel, S. Tamm, L. Olsson, T.S. Khan, T. Bligaard, P. Gabrielsson, and S. Dahl, *Appl. Catal. B* 2011, Accepted Manuscript, doi: 10.1016/j.apcatb.2011.11.042

- [17] S. Fogel and D.E. Doronkin, et. al. Manuscript in preparation
- [18] REGULATION (EC) No 715/2007 OF THE EUROPEAN PARLIAMENT AND OF THE COUNCIL of 20 June 2007, Official Journal of the European Union, (29.6.2007), L 171/1 – L 171/16
- [19] “VOLVO S80 Instruktionsbok Web Edition” [http://esd.volvocars.com/site/owners-information/MY11/S80/PDF/S80\\_owners\\_manual\\_MY11\\_SE\\_tp11740.pdf](http://esd.volvocars.com/site/owners-information/MY11/S80/PDF/S80_owners_manual_MY11_SE_tp11740.pdf) (accessed Jun 2011)
- [20] G.M. Wallace, ”EUROPEAN DIESEL FUEL - A REVIEW OF CHANGES IN PRODUCT QUALITY 1986-1989”, Preprint archive of the ACS Division of Fuel Chemistry, Vol 35(4) (1990) 1080 – 1099
- [21] DIRECTIVE 2009/30/EC OF THE EUROPEAN PARLIAMENT AND OF THE COUNCIL of 23 April 2009, Official Journal of the European Union, (5.6.2009), L 140/88 – L 140/113
- [22] L. Olsson, H. Sjövall, and R.J. Blint, Appl. Catal. B 81 (2008) 203-217
- [23] A. Sultana, M. Haneda, T. Fujitani, and H. Hamada, Catal. Lett. 114 (2007) 96-102
- [24] K.-I. Shimizu, J. Shibata, H. Y., A. Satsuma, T. Hattori, Appl. Catal. B 30 (2001) 151–162
- [25] Q. Wu, H. Gao, and H. He, J. Phys. Chem. B 110 (2006) 8320-8324
- [26] I. Levin and D. Brandon, J. Am. Ceram. Soc., 81 (1998) 1995–2012
- [27] R. Burch, J.P. Breen, and F.C. Meunier, Appl. Catal. B 39 (2002) 283–303
- [28] T.C. Brüggemann, D.G. Vlachos, F.J. Keil, J. Catal. 283 (2011) 178-191
- [29] B. Hammer, J.K. Nørskov, Adv. Catal. 45 (2000) 71-129
- [30] B. Hammer, O.H. Nielsen and J.K. Nørskov, Catalysis Letters 46 (1997) 31-35
- [31] Á. Logadóttir, J.K. Nørskov, Journal of Catalysis 220 (2003) 273–279
- [32] Ton V. W. Janssens, Bjerne S. Clausen, Britt Hvolbæk, Hanne Falsig, Claus H. Christensen, Thomas Bligaard, and Jens K. Nørskov, Topics in Catalysis 44, (2007), 15-26



- [33] N. Jagtap, S.B. Umbarkar, P.Miquel, P. Granger , and M.K. Dongare, Appl. Catal. B 90 (2009) 416–425
- [34] B. Kartheuser, B. K. Hodnett, Alfredo Riva, G. Centi, H. Matralis, M. Ruwet, Paul Grange, and N. Passarini, Ind. Eng. Chem. Res. 30 (1991) 2105-2113

## Figure legends

**Figure 1.** NO<sub>x</sub> (a) and NH<sub>3</sub> (b) conversion profiles obtained over fresh 1 - 3% Ag/Al<sub>2</sub>O<sub>3</sub> (black) and hydrothermally aged 1% Ag/Al<sub>2</sub>O<sub>3</sub> (gray dotted) catalysts.

(c) Evolution of NO<sub>x</sub> conversion at 227 and 250 °C over 2% Ag/Al<sub>2</sub>O<sub>3</sub> with 10 ppm SO<sub>2</sub> in the feed.

(d) NO<sub>x</sub> and NH<sub>3</sub> conversion profiles obtained over sulfur poisoned 1 - 3% Ag/Al<sub>2</sub>O<sub>3</sub> catalysts.

(e) NO<sub>x</sub> and NH<sub>3</sub> conversion profiles obtained over 1 - 3% Ag/Al<sub>2</sub>O<sub>3</sub> catalysts after 40 min. regeneration at 670 °C.

Reaction conditions: 500 ppm NO, 520 ppm NH<sub>3</sub>, 1200 ppm H<sub>2</sub>, 8.3% O<sub>2</sub>, 7% H<sub>2</sub>O in Ar, GHSV = 110 000 h<sup>-1</sup>.

**Figure 2.** (a) NO<sub>x</sub> conversion profiles obtained over 2% Ag/Al<sub>2</sub>O<sub>3</sub> after 10 min.

regeneration at 670 °C (dashed) and after 1 min. regeneration at 670 °C in rich mixture (solid). Reaction conditions: 500 ppm NO, 520 ppm NH<sub>3</sub>, 1200 ppm H<sub>2</sub>, 8.3% O<sub>2</sub>, 7% H<sub>2</sub>O in Ar, GHSV = 110 000 h<sup>-1</sup>.

(b) Dependence of shift of temperature of 50% NO<sub>x</sub> conversion on the regeneration time. The 0 corresponds to no regeneration.

**Figure 3.** (a) Temperature profile of 4 h. sulfation – 40 min. regeneration experiment.

(b) Temperature profile of 4 x 1 h. sulfation – 10 min. regeneration experiment.

(c) NO<sub>x</sub> conversion profiles obtained over fresh 2%Ag/Al<sub>2</sub>O<sub>3</sub> (solid line), 2%Ag/Al<sub>2</sub>O<sub>3</sub> after 4 h. with 10 ppm SO<sub>2</sub> at 240 °C and 40 min. regeneration at 670 °C (dotted line), after 4 cycles 1 h. with 10 ppm SO<sub>2</sub> at 240 °C and 10 min. regeneration (dashed line).

**Figure 4.** Evolution of NO<sub>x</sub> conversion with time for first 9 cycles of the long term stability test of 2%Ag/Al<sub>2</sub>O<sub>3</sub>. Reaction conditions: 500 ppm NO, 1200 ppm H<sub>2</sub>, 8.3% O<sub>2</sub>, 7% H<sub>2</sub>O in Ar, GHSV = 110 000 h<sup>-1</sup>. Sulfation with 10 ppm SO<sub>2</sub> for 1 h. at 240 °C, regeneration for 10 min. at 670 °C.

**Figure 5.** The scheme of Ag/Al<sub>2</sub>O<sub>3</sub> sulfation and regeneration.

**Figure 6. (a)** NO<sub>x</sub> conversion profiles obtained over fresh 2%Ag/Al<sub>2</sub>O<sub>3</sub> (solid line), 2%Ag/Al<sub>2</sub>O<sub>3</sub> after 4 h. with 10 ppm SO<sub>2</sub> at 240 °C, followed by 40 min. regeneration at 670 °C (dotted line) and after additional regeneration at 950 °C (dashed line).

**(b)** Temperature dependence of NO<sub>2</sub> concentration at the reactor outlet obtained over fresh 2%Ag/Al<sub>2</sub>O<sub>3</sub> (solid line), 2%Ag/Al<sub>2</sub>O<sub>3</sub> after 4 h. with 10 ppm SO<sub>2</sub> at 240 °C, followed by 40 min. regeneration at 670 °C (dotted line) and after additional regeneration at 950 °C (dashed line). Reaction conditions: 500 ppm NO, 520 ppm NH<sub>3</sub>, 1200 ppm H<sub>2</sub>, 8.3% O<sub>2</sub>, 7% H<sub>2</sub>O in Ar, GHSV = 110 000 h<sup>-1</sup>.

**Figure 7.** The most energetically favorable adsorption geometries for adsorption of SO<sub>2</sub>, SO<sub>3</sub>, and SO<sub>4</sub> on γ-Al<sub>2</sub>O<sub>3</sub> model surface (with corresponding adsorption energies).

**Table 1.** Specific surface areas of tested catalysts as measured by BET.

Catalyst	Treatment	S <sub>BET</sub> [m <sup>2</sup> /g]
1% Ag/Al <sub>2</sub> O <sub>3</sub>	-	142
1% Ag/Al <sub>2</sub> O <sub>3</sub>	hydrothermal aging (750 °C, 16 h.)	126
2% Ag/Al <sub>2</sub> O <sub>3</sub>	catalytic test (w/o deactivation)	130
2% Ag/Al <sub>2</sub> O <sub>3</sub>	sulfation and 10 min. regen. @ 670 °C	129
2% Ag/Al <sub>2</sub> O <sub>3</sub>	sulfation and 80 min. regen. @ 670 °C	113
2% Ag/Al <sub>2</sub> O <sub>3</sub>	30 cycles of 1h. sulfation and 10 min. regen. @ 670 °C, followed by heating to 950 °C	121
3% Ag/Al <sub>2</sub> O <sub>3</sub>	-	141

**Table 2.** Adsorption energies and desorption temperatures of SO<sub>x</sub> for the most energetically favorable adsorption geometries in case of different adsorption sites.

	Type II (metallic Ag)				Type I (dispersed Ag)					
	Ag (111)		Ag (211)		$\gamma$ -Al <sub>2</sub> O <sub>3</sub>		Ag built in the $\gamma$ -Al <sub>2</sub> O <sub>3</sub> surface		Ag on the step of $\gamma$ -Al <sub>2</sub> O <sub>3</sub>	
	E <sub>ads</sub> , eV	T <sub>des</sub> , K	E <sub>ads</sub> , eV	T <sub>des</sub> , K	E <sub>ads</sub> , eV	T <sub>des</sub> , K	E <sub>ads</sub> , eV	T <sub>des</sub> , K	E <sub>ads</sub> , eV	T <sub>des</sub> , K
SO <sub>2</sub>	not adsorbed		-0.26	81	-1.43	558	-2.06	791	-1.29	506
SO <sub>3</sub>	-1.61	390	-1.82	458	-2.66	630	-3.34	781	-2.64	625
SO <sub>4</sub>	-2.65	454	-2.97	597	-1.15	222	-1.77	331	-3.14	572

**Table 3.** Energies of HSO<sub>x</sub> species in the gas phase and adsorbed on the most energetically favorable adsorption sites.

Energy*, eV :	HSO <sub>2</sub>	HSO <sub>3</sub>	H <sub>2</sub> SO <sub>3</sub>	HSO <sub>4</sub>	H <sub>2</sub> SO <sub>4</sub>
Gas phase	0.29	-	-	-1.48	-3.39
Adsorbed on $\gamma$ - Al <sub>2</sub> O <sub>3</sub>	Dissociates	-2.84	Dissociates	-3.16	Dissociates
Adsorbed on Ag built in the $\gamma$ - Al <sub>2</sub> O <sub>3</sub>					
Adsorbed on Ag (211)	0.02	Dissociates	-2.22	-3.94	-3.57

\* Energy of the HSO<sub>x</sub> species is given with respect to SO<sub>2</sub> (g), O<sub>2</sub> (g) and H<sub>2</sub> (g).

Figure 1

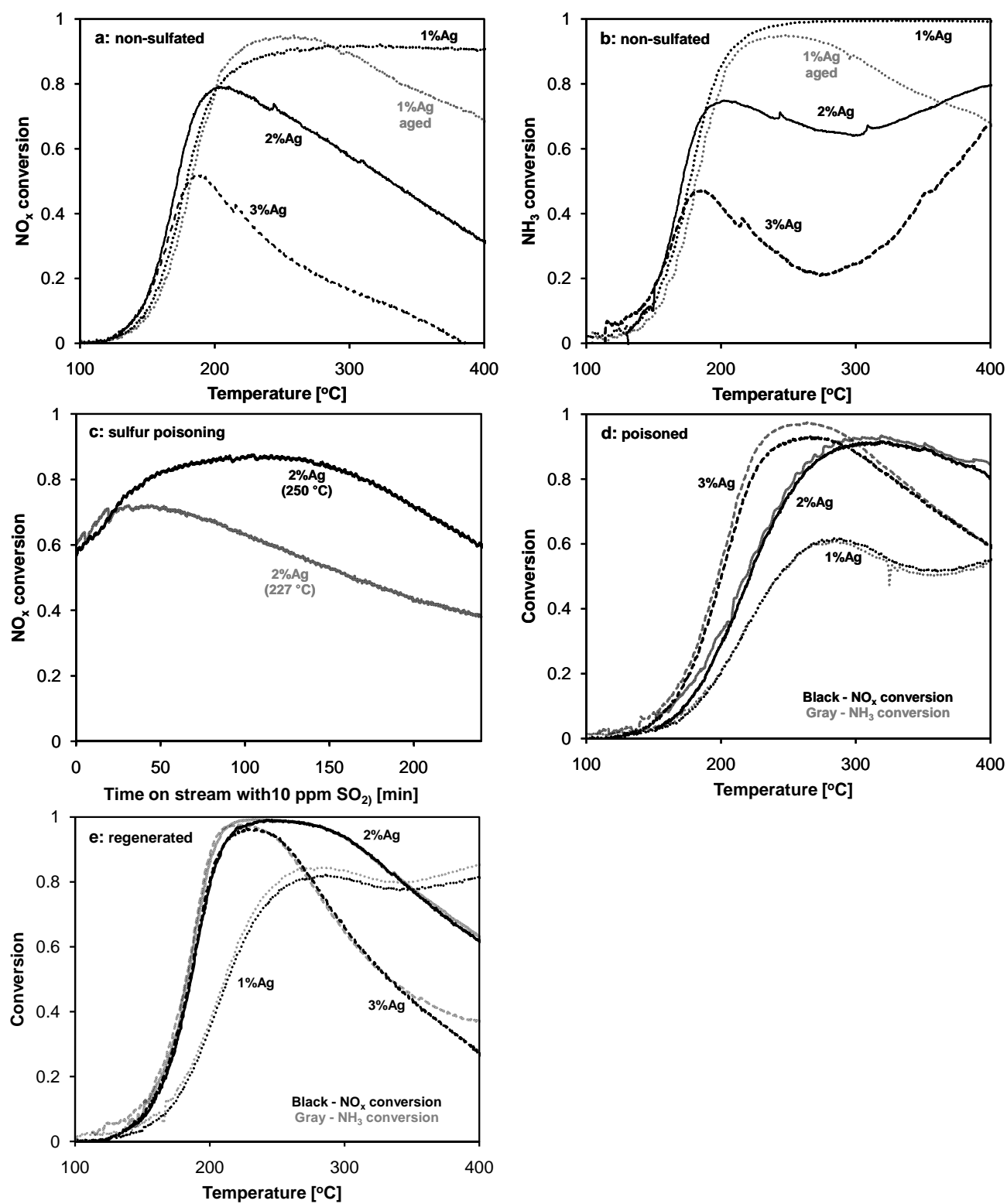


Figure 2

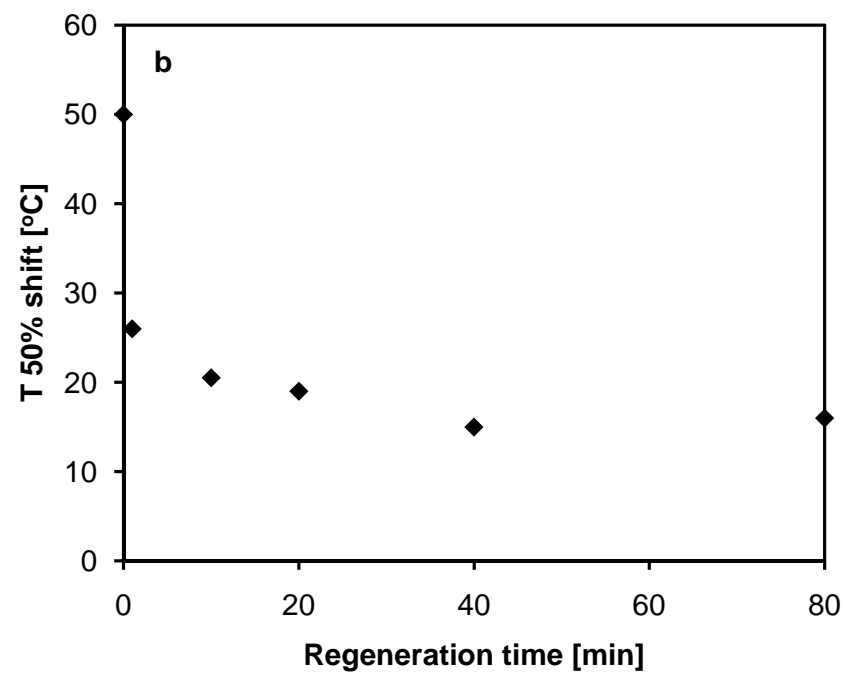
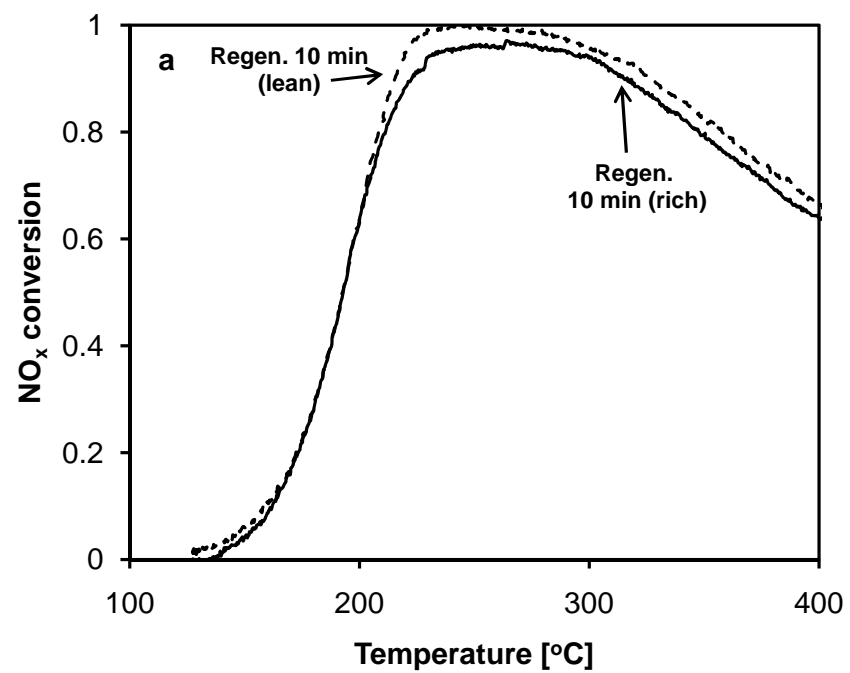




Figure 3

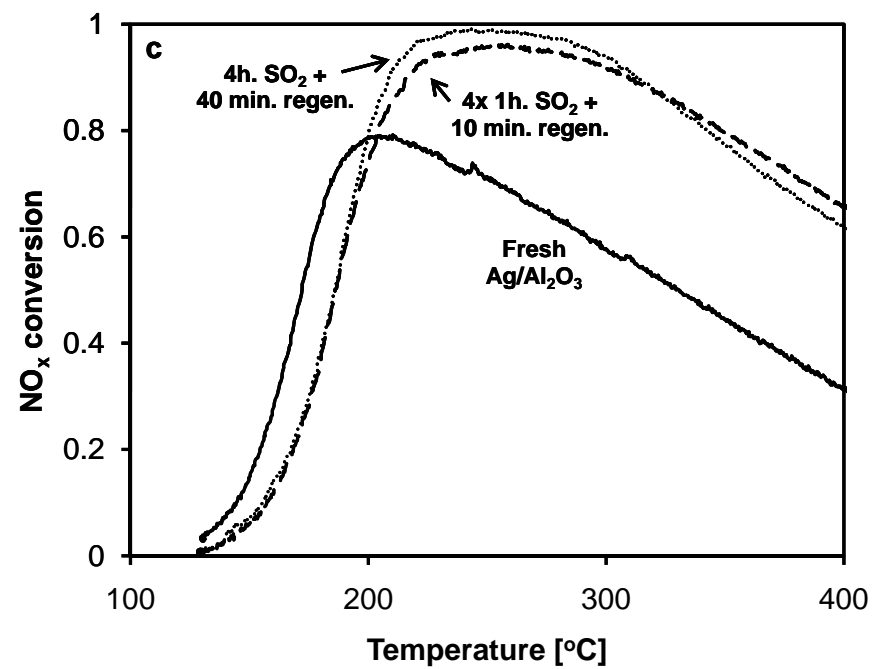
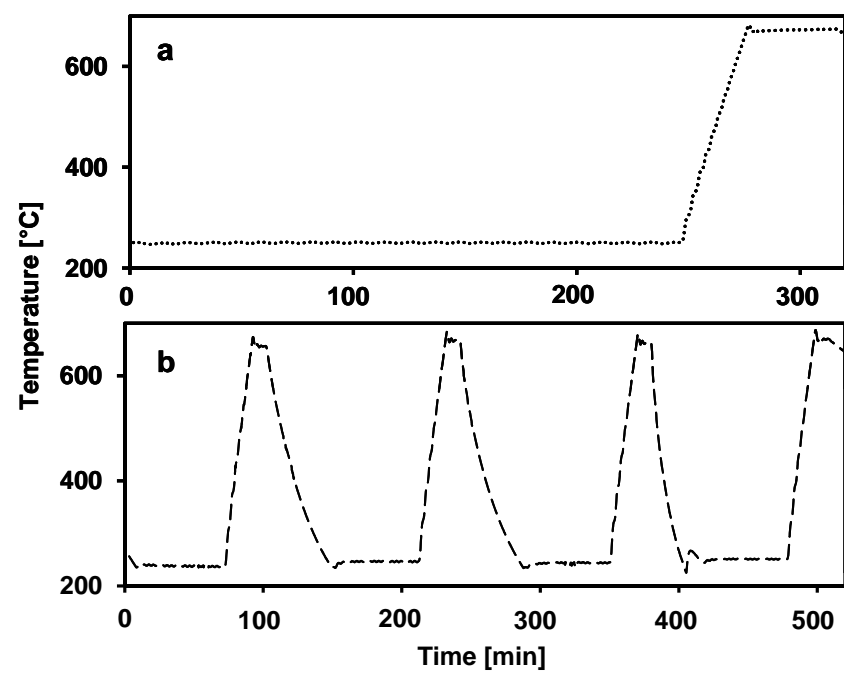


Figure 4

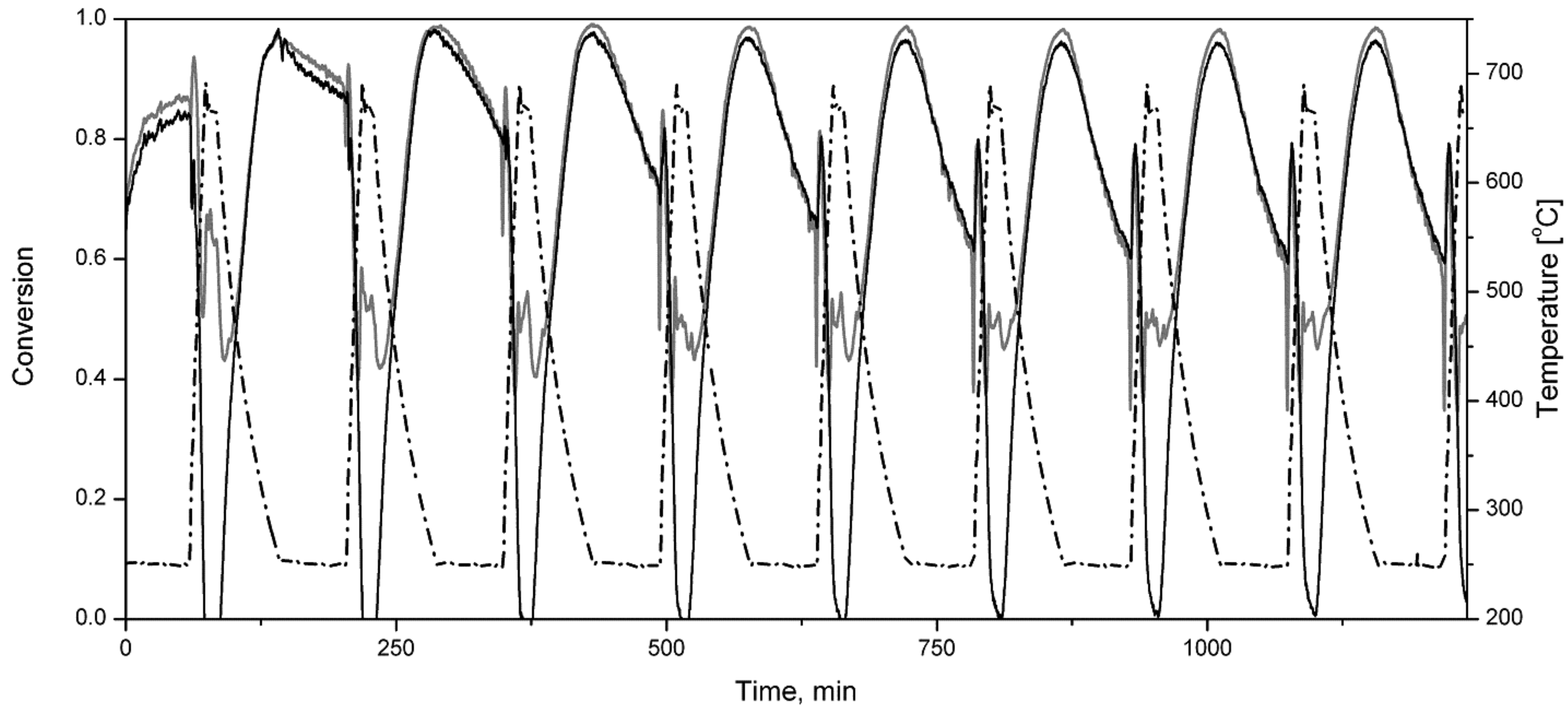


Figure 5

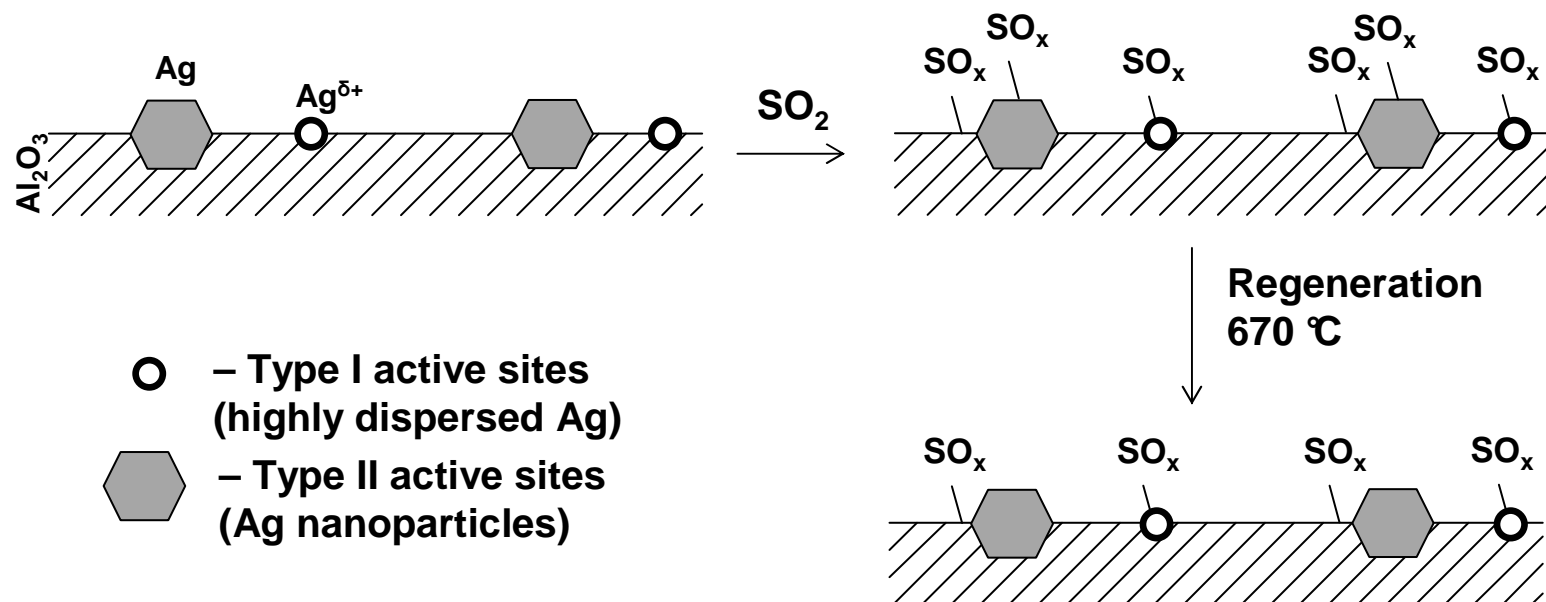


Figure 6

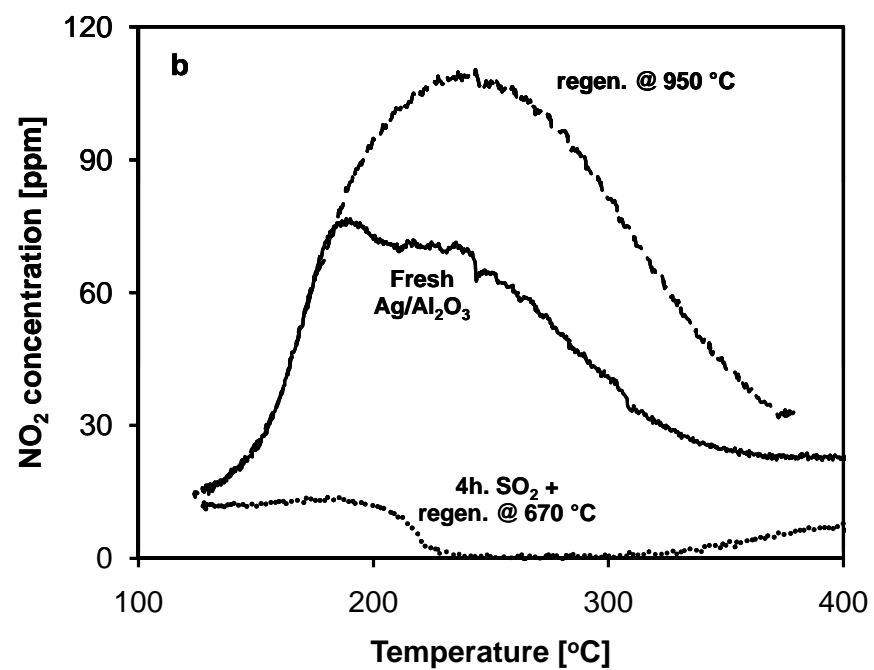
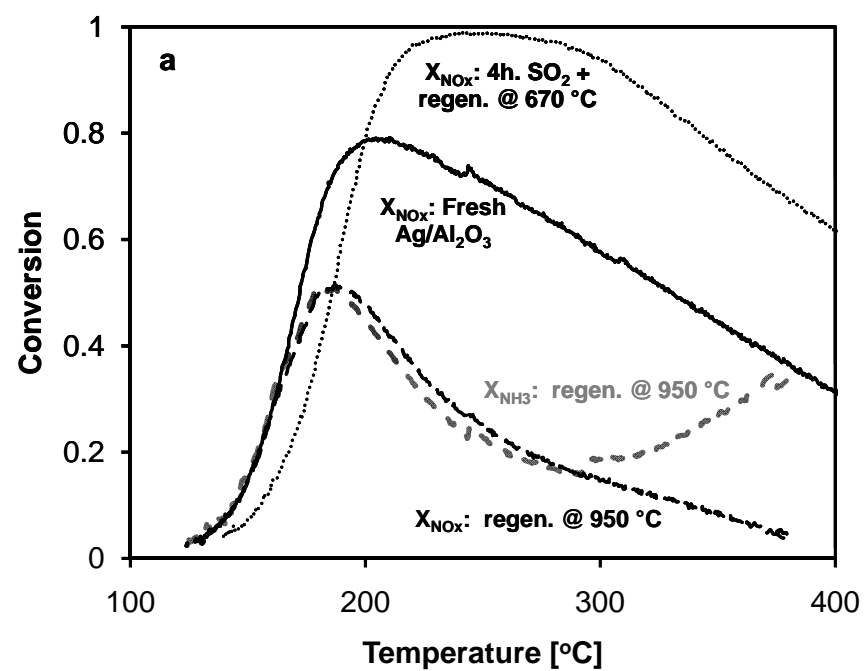
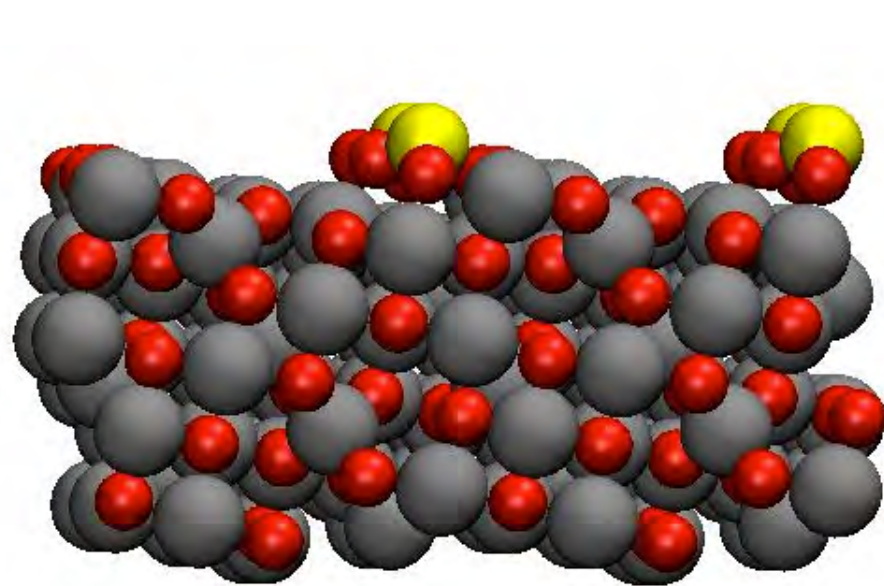
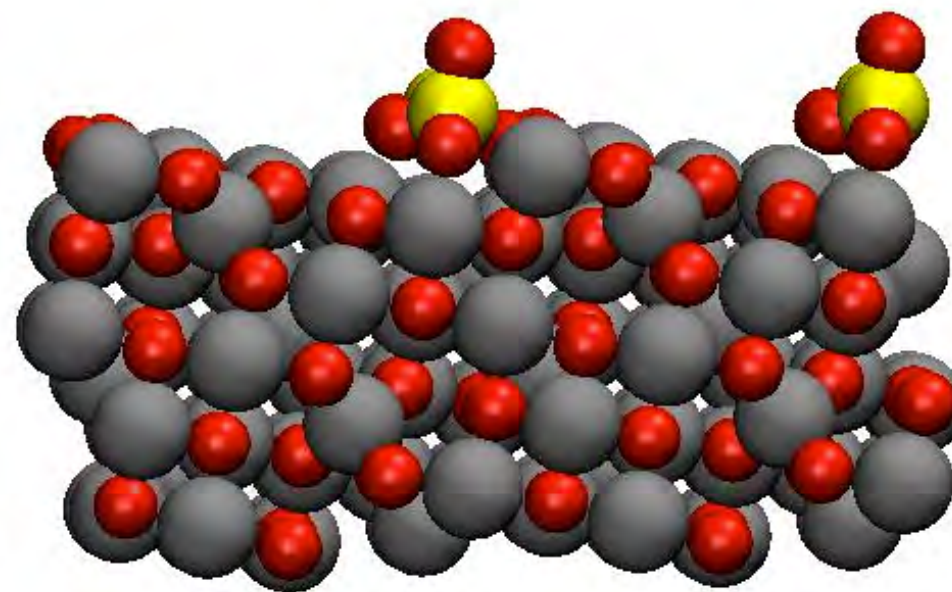


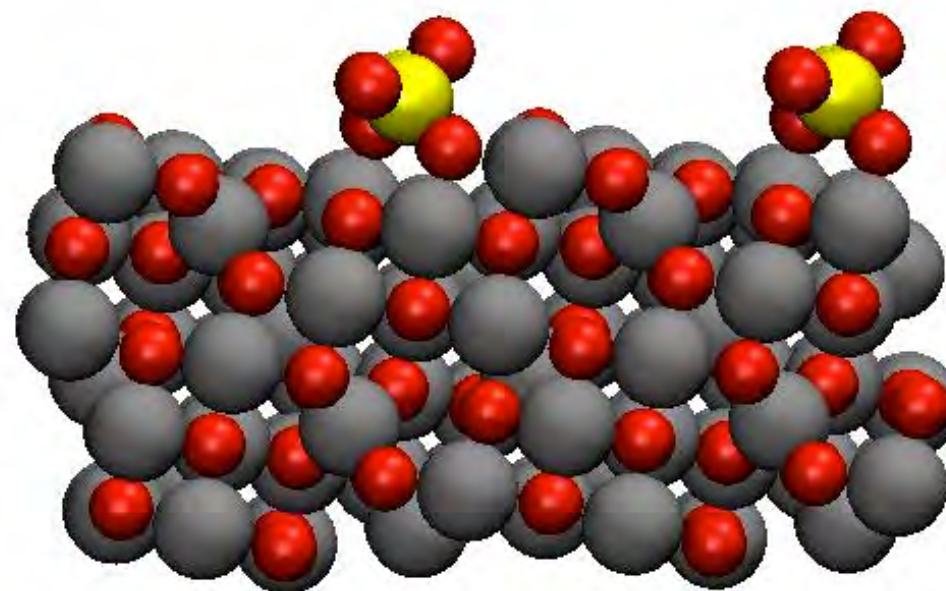
Figure 7



$\text{SO}_2 @ \gamma\text{-Al}_2\text{O}_3$ : -1.43 eV



$\text{SO}_3 @ \gamma\text{-Al}_2\text{O}_3$ : -2.66 eV



$\text{SO}_4 @ \gamma\text{-Al}_2\text{O}_3$ :  
-1.15 eV